Enhanced Pinning with Controlled Splay Configurations of Columnar Defects; Rapid Vortex Motion at Large Angles

L. Krusin-Elbaum,[1] A. D. Marwick,[1] R. Wheeler,[2] C. Feild,[1] V. M. Vinokur,[3] G. K. Leaf,[3] and M. Palumbo[4]
[1]*IBM Research, Yorktown Heights, New York 10598*
[2]*The Ohio State University, Columbus, Ohio 43210*
[3]*Argonne National Laboratory, Argonne, Illinois 60439*
[4]*Physikalisches Institut, Universitat Bayreuth, D-8580 Bayreuth, Germany*
(Received 27 September 1995)

Orders-of-magnitude enhancements of persistent currents J are reported in $YBa_2Cu_3O_{7-\delta}$ with columnar defects arranged in a variety of splayed configurations. The largest J is obtained for a planar distribution $P_{pl}(\Theta)$, with a splay angle $\Theta_{opt} = \pm 5^\circ$. A comparison of $P_{pl}(\Theta)$ and a Gaussian distribution $P_G(\Theta)$ suggests that pinning by the latter is controlled by large-angle tails of the Gaussian which appear to *enhance* thermal creep rate. Numerical simulations confirm the existence of the regimes where vortex motion is *promoted* rather than *suppressed* by splay.

PACS numbers: 74.60.Ge, 74.60.Jg, 74.62.Dh

Pinning of magnetic vortices in the mixed state of a type-II superconductor is unarguably optimized with linear defects [1]. In cuprate superconductors, an effective defect structure consisting of a random array of nearly parallel columns of amorphized material, $\sim 50-80$ Å in diameter, can be installed by the irradiation with swift (~ 1 GeV) heavy ions, such as Pb, Sn, or Au [2,3]. In a highly anisotropic (but three-dimensional) $YBa_2Cu_3O_{7-\delta}$ (YBCO), the resulting pinning is strongest when the magnetic field is aligned with defects [2]—tilting the field beyond the trapping angle [1,4] reduces both the critical current density J_c and the strong pinning range [1,2].

It has been proposed by Hwa *et al.* [5] that pinning and thus transport properties can be further improved by a dispersion (splay) in track directions. In the theory of [5], there are two major mechanisms reducing the flux motion: first, the vortex entanglement [6], forced by vortex localization on splayed tracks; second, the variable range vortex transport at low currents [4], which should be suppressed by splay since the *dominant excitations* [via double (super)kinks [4,5]] *are expected to occur within the families of similarly inclined tracks.* On the other hand, in discussing the strategies for improving transport one should keep in mind that splay may *promote* flux motion. It was already noted that too large splay angles with reduce the irreversible regime [5]. Another effect can arise from splayed tracks intersecting each other. The action of the crossings (or close encounters) is twofold. They can serve as additional pinning sites for the vortex kinks moving along the defect of the vortex original habitat [5], impeding the vortex from wandering off its track, and, therefore, suppressing vortex creep. But, the crossings could also induce kink nucleation, i.e., allow for easier vortex jumps from one track to another, giving rise to "zigzag" configurations which may *stimulate* creep. The outcome of the competition between the suppression and promotion mechanisms should depend, among others, on the driving force, field, temperature, and the number of crossings; thus, the optimal pin configuration may depend on the regime under consideration.

Recently, we have established the effectiveness of the uniform splay which can be installed with fission in a quasi-2D $Bi_2Sr_2CaCu_2O_{8+\delta}$ (BSCCO), a structure of possible technological relevance [7]. And, we found a slower vortex dynamics in YBCO crystals when a splay, naturally occurring in the irradiation process [8], is larger. Yet, the optimal pinning configuration for a 3D material is still to be found.

Here, we report orders-of-magnitude enhancement of the persistent current density J in irradiated YBCO crystals for several *controlled* splay configurations of columnar defects, exceeding J for the parallel tracks. We also demonstrate the existence of regimes where splay *enhances* vortex dynamics, showing that the optimal pin configuration is regime specific. We explore Gaussian, $P_G(\Theta)$, and planar, $P_{pl}(\Theta)$, splay distributions of two parallel pin families crossing each other at a variety of angles. For a planar splay, we establish an *optimal relative splay angle* $\Theta_{opt} = 10^\circ$, for which J is significantly enhanced above that of the parallel configuration, $P_\parallel$. A Gaussian splay appears *less effective than the parallel configuration.* Large vortex creep for $P_G(\Theta)$ is thought to be *driven by the large-angle tails* of the Gaussian, by generating numerous intersections of tracks. Faster dynamics at large Θ is confirmed in numerical simulations.

Several YBCO crystals of ~ 1 mm size and 15 to 20 μm thick along the **c** axis were irradiated with 1.08 GeV $^{197}Au^{23+}$ at the TASCC facility at Chalk River Laboratories in Canada [9]. To install planar splay, the ion beam was tilted off the $\mathbf{c}(\hat{z})$ axis by rocking the crystals about an axis $\perp \hat{z}$ (as sketched in Fig. 1) by $\pm\Theta$ in a range from 2.5° to 15°. A representative cross-sectional transmission electron microscopy (TEM) image of a crystal with a planar splay is shown in Fig. 1. Gaussian splay was obtained by irradiating ~ 15 μm thick crystals through a 5 μm thick Au foil. The full width at

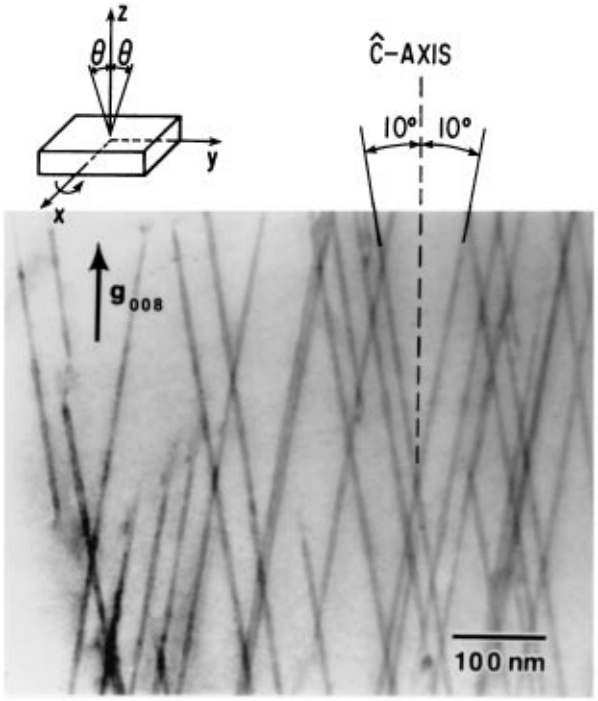

FIG. 1. Cross-sectional TEM image of YBCO irradiated with 1.08 GeV Au, taken from a region at ≈9 μm from the entry surface of a ~19 μm thick crystal. This crystal was rocked around an axis ⊥ **c** (upper left sketch) by an angle $\Theta = \pm 10$. The viewing direction is nearly along the axis of ±10° rotation (i.e., ~ along [010]).

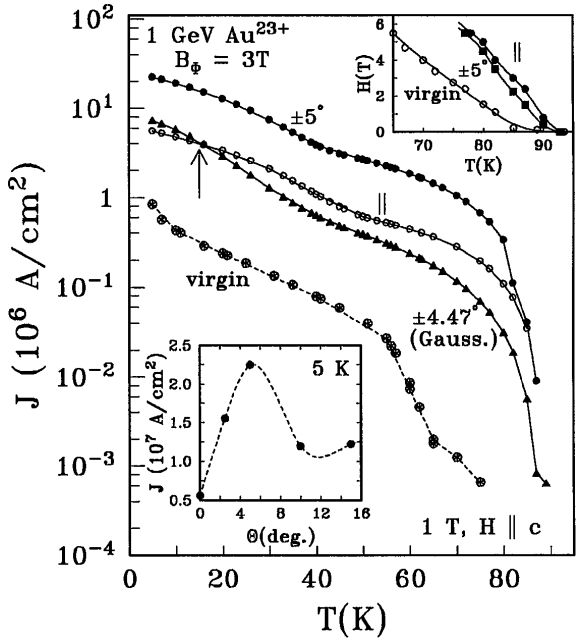

FIG. 2. Persistent current density $J(T)$ for YBCO crystals with three splay configurations of columnar pins, each with $B_\Phi = 3$ T: planar splay (solid dots) with $\Theta = \pm 5°$, parallel tracks (open circles), and a Gaussian distribution (solid triangles) with FWHM of ±4.47°. The best result is for the ±5° planar splay (also lower inset). $J(T)$ for the same crystal before irradiation (encircled stars) is also shown. $H_{\rm irr}(T)$ is shifted to higher temperatures after irradiation (upper inset). $J(T)$ for the Gaussian splay is *smaller* than for the ∥ pins above ~16 K (the arrow).

half maximum (FWHM) of $P_G(\Theta)$ was estimated from the TRIM Monte Carlo calculations [8,10]. The ion energy was ~0.6 GeV at the entrance to crystals, setting the projected range at ~21 μm [10]. The energy deposition rate was above the threshold for columnar track formation (1.8 keV/Å) throughout the crystal thickness [8,10,11]. In all cases, the total pin density corresponded to a dose-equivalent matching field $B_\Phi = 3$ T.

Figure 2 shows the temperature variation of persistent currents $J(T)$ for different configurations of columnar pins in a field of 1T applied along the **c** axis. $J(H,T)$ was obtained from the irreversible magnetization $M(H,T)$ in the critical state [12], measured with a SQUID magnetometer [7,8]. The variation in J in crystals before irradiation was less than 20% [2,8]. Inspection of a crystal with $P_{\rm pl}(\pm 5°)$ and the *same* (virgin) crystal before irradiation shows that after irradiation $J(5\ {\rm K}) \cong 2 \times 10^7\ {\rm A/cm^2}$—an increase by over an order of magnitude. The enhancement at 77 K is by about 4 *orders of magnitude.* A maximum in $J(\Theta)$, shown in the lower inset of Fig. 2, indicates that the ±5° planar splay supports the largest current, well above the parallel (∥) configuration. At the same time the strong pinning range is nearly intact. Both the ∥ and ±5° pins shift the irreversibility line, $H_{\rm irr}$, towards high temperatures in a predictable way [9], as shown in the upper inset of Fig. 2. A slight downward displacement of $H_{\rm irr}(T)$ for the ±5° splay, relative to $P_\parallel$, is expected from the decrease of glass melting temperature due to the average tilt [5].

Intuitively, one might expect a greater degree of entanglement for a Gaussian splay [5], and thus the largest J_c. This is not observed. $J(T)$ for $P_G(\Theta)$ with ±4.47° FWHM (Fig. 2) falls *below parallel configuration* above $T \simeq 16$ K. The detrimental effect of large-angle tails of $P_G(\Theta)$ is suggested by the different field dependencies of $J(H,T)$ for the Gaussian and planar (or $P_\parallel$) arrangements. It is particularly striking at high temperatures. At 70 K, $J(H)$ for the parallel-pin and planar-splay arrangements for sufficiently small (<45°) angles, *all* give a distinct "dip" in $J(H)$ around zero field [Fig. 3(a)], which articulates above 40 K and disappears near T_c. $J(H)$ for the Gaussian has a spike-like feature near $H \cong 0$. Such shape difference was seen in $M(H)$ for $H \parallel$ defects and H misaligned with defects by a large (60°) angle in the experiment of Civale *et al.* [2] (Fig. 3 inset).

The effect on vortex dynamics is shown in Fig. 3(b), which contrasts the thermal relaxation rates $S = -d\ln J/d\ln t$ for the Gaussian, the ±5°, and the ∥ pin configurations. $S(H,T)$ was obtained from the time evolution of $M(H,T,t)$ from the critical state for times $60 < t < 7200$ sec [13]. Below $H \sim 1.5$ T and outside

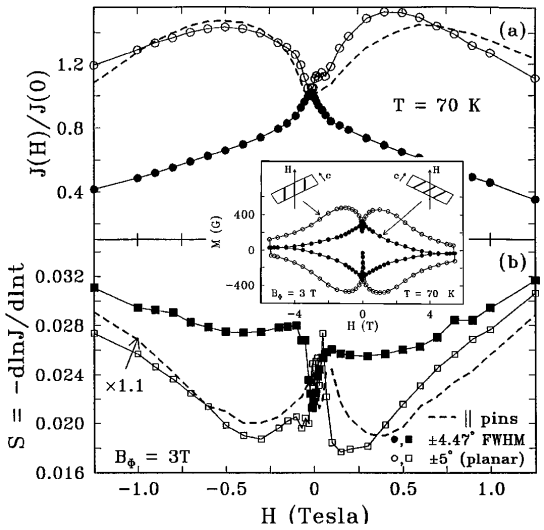

FIG. 3. (a) $J(H)$ at $T = 70$ K for the ∥ pins, $\pm 5°$ splay, and a Gaussian splay with $\pm 4.47°$ FWHM. (b) Corresponding normalized creep rates S for the same three crystals. Except near $H \sim 0$, the creep is measurably larger for the Gaussian in this field range. Inset illustrates the shape difference of $M(H)$ at 70 K for H ∥ defects and misaligned by 60° (from Ref. [2]), suggesting the controlling role of large-angle tails of $P_G(\Theta)$.

a narrow region near $H \cong 0$, the *creep rate is faster for the Gaussian splay*—it is 0.026 at $H \sim 0.25$ T, as compared with 0.018 for a $\pm 5°$ arrangement. For ∥ pins and $\pm 5°$ splay the creep rates are comparable.

The data in Fig. 3 suggest similar dominant pinning mechanism for the large-angle defect-field misalignment in Civale's experiment [2] and for the Gaussian splay. Namely, pinning of the kinks [14] generated by either the *vortex-defect* [2,15] or *defect-defect* intersections. For the tilted defects [2] shown here, the kink pinning is presumably by the track inhomogeneities [2]. For the splayed pins, especially for the Gaussian and large-angle planar configurations, it is by defect-defect crossings. These crossings play a dual role. We view each family of parallel tracks as the valleys in the (nonperiodic) "washboard" potential. The intersections of the given family with another one (or with the differently angled tracks) *locally* lower the barrier, easing the way for the vortex to escape. A similar effect was observed in numerical studies of the motion of the *dislocations* in semiconductors through the periodic washboard (Peierls) potential in the presence of point disorder [16]. The dislocation motion occurs via the same nucleation process as the escape of the vortex from a given track (or the hopping between the adjacent tracks). The point defects in this case were found not only to retard the kink propagation along the dislocation line, but also to locally depress the barrier between the adjacent valleys, easing a way for a dislocation to make a nucleus-like configuration.

To gain insight into the scenario proposed above we investigated numerically vortex motion through the planar splay configurations of columnar defects. We considered a sample of thickness L along the $\hat{z}$ direction and an infinite lateral extent with an external magnetic field along $\hat{z}$. A single flux line was then parametrized by a set of two-dimensional vectors, $\mathbf{r}(z)$, which lie in a plane $\perp \hat{z}$.

The total free energy of the flux line is given by [1]

$$\mathcal{F} = \int_0^L dz \left[\varepsilon_0 \left(\frac{d\mathbf{r}(z)}{dz} \right)^2 + U_p(\mathbf{r}(z), z) - \mathbf{F} \cdot \mathbf{r}(z) \right]. \tag{1}$$

Here ε_0 is the flux line tilt modulus, $U_p(\mathbf{r}(z), z)$ is an attractive pinning potential due to columnar pins of arbitrary orientation, and $\mathbf{F}$ is an external force.

The motion of the flux line defined by the discretized version of Eq. (1) through the random defect environment, at fixed temperature, was modeled via a Metropolis Monte Carlo scheme. All lengths were measured in units of the vortex core radius ξ, driving force F in units of ε_0/ξ, and pinning energy (per unit length) and temperature T in units of ε_0 and $\varepsilon_0\xi$, respectively. U_p was modeled as a smooth-edged cylindrical parabolic well of depth $U_0 = 1$ and radius $R = 2$. We simulated single-vortex motion through the system of columnar defects parallel to magnetic field and through the families of $\pm 10°$ and $\pm 45°$ planar splay configurations of identical randomly positioned columnar pins. The total density of defects was taken to be $\rho = 0.2$, and $T = 0.5$ [17]. Each vertical line segment was randomly kicked (in turn) with the variation in energy $\delta\mathcal{F}$ for each kick calculated with Eq. (1). Any step which decreased $\mathcal{F}$ was automatically accepted, while a step that increased $\mathcal{F}$ had a probability $P = \exp(-\delta\mathcal{F}/T)$ of being accepted. A typical run could involve 20×10^6 Monte Carlo sweeps through a string of vertical length $N_z = 128$, with the string's average position sampled every 4×10^3 sweeps.

The results of the simulation are shown in Fig. 4. The vortex velocity v for the $\pm 45°$ splay clearly exceeds that for the ∥ pins and for the $\pm 10°$ splay. This supports our expectation that the vortex motion can be significantly stimulated by the formation of zigzags; this effect should be larger for the $\pm 45°$ splay due to a greater number of intersections. The log-log plot of v vs F is well described by $v \propto \exp(-\text{const}/F^{\mu})$, characteristic of the glassy vortex motion [1]. The upper inset shows exponents μ for ∥ defects and for the $\pm 10°$ planar splay. For parallel pins $\mu = 0.8 \pm 0.2$, in good agreement with the predicted value $\mu = 1$ for the half-loop vortex creep regime [4]. It is important to note that $\mu = 1.4 \pm 0.2$ for the $\pm 10°$ splay implies that at sufficiently small driving forces the velocity through the $\pm 10°$ splay will become *less* than in the system with parallel pins [18].

Although it is not trivial to project the above simulation results to large fields, we expect the crossovers from nucleation dominated to kink pinning dominated creep to occur there as well. An experimental crossover is

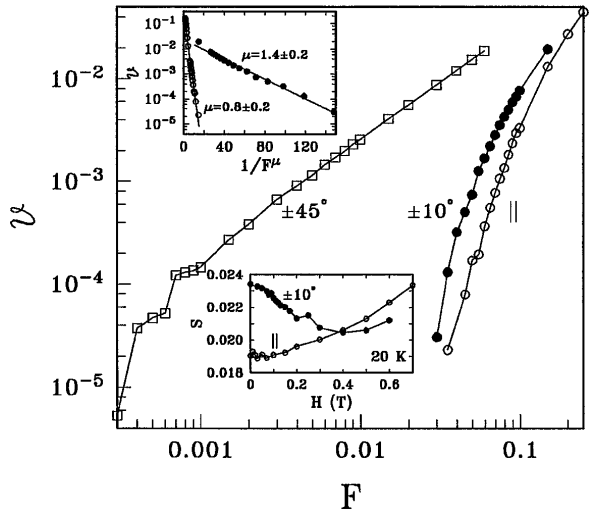

FIG. 4. Vortex velocity v vs driving force F from the Monte Carlo simulations (see text) for parallel pins, and for planar splay with $\Theta = \pm 10°$ and $\pm 45°$. The results are equivalent to the *V-I* curves, with voltage $\propto v$ and $F \propto$ current. The values of the glassy exponent μ (upper inset) for the $\|$ and $\pm 10°$ splayed pins indicate that a crossover in v will occur at lower forces. Lower inset: An experimental crossover to the suppression of creep by splay for the same pin configurations.

shown in the lower inset of Fig. 4. At 20 K near $H \sim 0$, the creep rate is indeed larger for the $\pm 10°$ splay than for the $\|$ defects. A crossover to suppression of creep by the $\pm 10°$ splay occurs at 0.4 T field. For this Θ, a second (reverse) crossover is observed at $H \sim 1$ T, shown in Fig. 5, which displays creep rate $S(H)$ for four defect configurations. The rate is largest for the Gaussian, consistent with the faster dynamics at large angles—at low fields it is *twice that of parallel pins.* Near $H \sim 0$, S is *lowest for the parallel pins.* At a higher field the creep rates *cross.*

Note that even the simplest cases of creep of an individual vortex line or a dislocation [16] reveal very

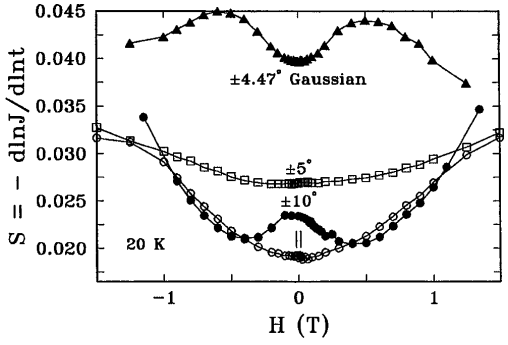

FIG. 5. Normalized creep rate $S(H)$ at $T = 2$ K for four YBCO crystals with different pin configurations. It clearly shows the regimes where vortex motion is promoted rather than suppressed by splay. Creep is fastest for the Gaussian. At 20 K, $S(H)$ for the $\pm 5°$ splay becomes lowest above 1 T.

complicated *nonlinear* and *nonadditive* nature of the competition between kink nucleation and kink pinning. In finite magnetic fields, when vortex-vortex interactions are relevant [1], the outcome will nontrivially depend on temperature, time, and B_Φ. In particular, the creep energy barriers and J_c may not be directly related, as reflected in our data. In conclusion, our results clearly establish that very large current enhancement can be obtained with splayed columnar defects. They also witness the existence of the regimes where vortex motion is *promoted* rather than *suppressed* by splay.

We are pleased to acknowledge useful discussions with J. R. Thompson, P. LeDoussal, T. Hwa, and H. Kaper. The work of V. M. V. and G. K. L. was supported by the U.S. Department of Energy, BES-Material Sciences, under Contract No. W-31-109-Eng-38. We thank J. Hardy and J. Forster at TASCC-Chalk River, supported by AECL Research, for their help and the provision of irradiation facilities.

[1] G. Blatter *et al.,* Rev. Mod. Phys. **66**, 1125 (1994).
[2] L. Civale *et al.,* Phys. Rev. Lett. **67**, 648 (1991).
[3] M. Konczykowski *et al.,* Phys. Rev. B **44**, 7167 (1991); R. C. Budhani, M. Suenaga, and S. H. Liou, Phys. Rev. Lett. **69**, 3816 (1992).
[4] D. R. Nelson and V. M. Vinokur, Phys. Rev. Lett. **68**, 2398 (1992; Phys. Rev. B **48**, 13 060 (1993).
[5] T. Hwa, P. LeDoussal, D. R. Nelson, and V. M. Vinokur, Phys. Rev. Lett. **71**, 3545 (1993); (to be published).
[6] D. R. Nelson and S. Seung, Phys. Rev. B **39**, 9153 (1989).
[7] L. Krusin-Elbaum *et al.,* Appl. Phys. Lett. **64**, 3331 (1994).
[8] L. Civale *et al.,* Phys. Rev. B **50**, 4102 (1994).
[9] L. Krusin-Elbaum *et al.,* Phys. Rev. Lett. **72**, 1914 (1994).
[10] J. F. Ziegler, J. B. Biersack, and U. Littlemark, *The Stopping Range of Ions in Solids* (Pergamon Press, New York, 1985), p. 79.
[11] L. Civale *et al.,* (to be published) demonstrated pinning by columnar defects after irradiation with 0.312 GeV Au.
[12] A. M. Campbell and J. E. Evetts, Adv. Phys. **21**, 199 (1972).
[13] L. Civale, L. Krusin-Elbaum, J. R. Thompson, and F. Holtzberg, Phys. Rev. B **50**, 7188 (1994).
[14] The creep process can be viewed as a sequence of (i) kink nucleation (e.g., of half-loops) and (ii) kink propagation along the vortex line (further spreading of half-loops).
[15] Th. Schuster *et al.,* Phys. Rev. B **51**, 16 358 (1995).
[16] V. M. Vinokur and I. R. Sagdeev, Sov. Phys. Solid State **30**, 1566 (1988).
[17] The basic energy unit $\varepsilon_0 \xi$ is just the condensation energy in the volume ξ^3 times the small anisotropy factor ($\varepsilon_0 \xi \sim T_c$). For reasonable simulation times, the pin density must be fairly high to observe significant pinning.
[18] The smallest forces (currents) below $F_c\,(J_c)$ are not accessible to us due to the time constraints. Explicit crossovers were seen by H. Kaper (to be published) in a very high defect density splayed system with Gaussian distribution of pinning strengths.